

Catalysis Science & Technology

Accepted Manuscript



This is an *Accepted Manuscript*, which has been through the Royal Society of Chemistry peer review process and has been accepted for publication.

Accepted Manuscripts are published online shortly after acceptance, before technical editing, formatting and proof reading. Using this free service, authors can make their results available to the community, in citable form, before we publish the edited article. We will replace this *Accepted Manuscript* with the edited and formatted *Advance Article* as soon as it is available.

You can find more information about *Accepted Manuscripts* in the [Information for Authors](#).

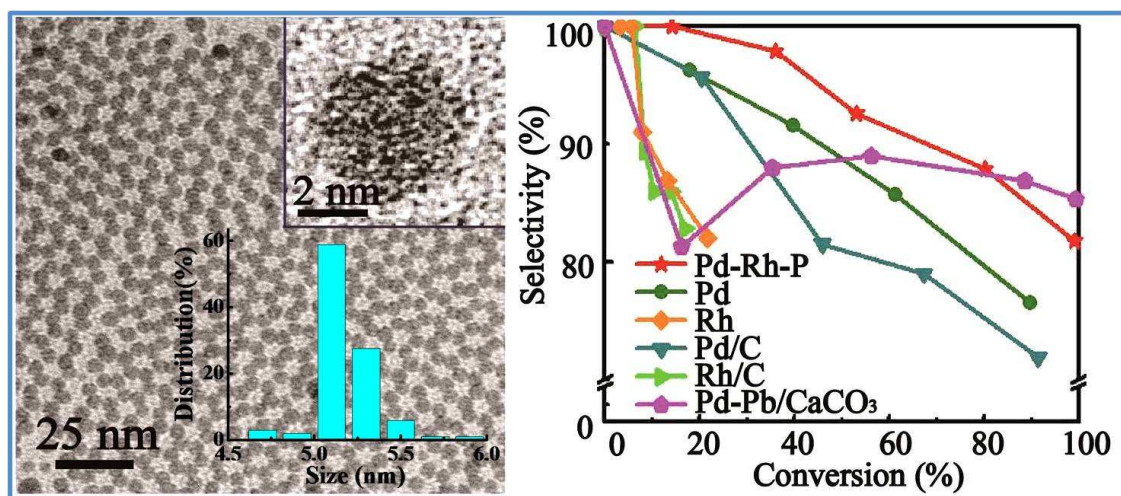
Please note that technical editing may introduce minor changes to the text and/or graphics, which may alter content. The journal's standard [Terms & Conditions](#) and the [Ethical guidelines](#) still apply. In no event shall the Royal Society of Chemistry be held responsible for any errors or omissions in this *Accepted Manuscript* or any consequences arising from the use of any information it contains.

Preparation of ternary Pd-Rh-P amorphous alloy and its catalytic performances toward selective hydrogenation of alkynes

Mengrui Ren, Changming Li, Jiale Chen, Min Wei,* Shuxian Shi*

State Key Laboratory of Chemical Resource Engineering, Beijing University of Chemical Technology, Beijing 100029, P. R. China

Graphical Abstract



Palladium-rhodium-phosphorus amorphous alloy nanoparticles were prepared *via* a facile one-pot synthesis method, which exhibit excellent catalytic behaviour toward selective hydrogenation of alkynes.

Cite this: DOI: 10.1039/c0xx00000x

www.rsc.org/xxxxxx

Communication

Preparation of ternary Pd-Rh-P amorphous alloy and its catalytic performances toward selective hydrogenation of alkynes

Mengrui Ren, Changming Li, Jiale Chen, Min Wei,* Shuxian Shi*

Received (in XXX, XXX) Xth XXXXXXXXX 20XX, Accepted Xth XXXXXXXXX 20XX

DOI: 10.1039/b000000

Palladium-rhodium-phosphorus amorphous alloy nanoparticles (~5.2 nm) were prepared via a facile one-pot synthesis method, which exhibit excellent catalytic behaviour toward selective hydrogenation of alkynes under mild conditions.

Alloy catalysts have recently attracted considerable attention in heterogeneous catalysis,¹⁻³ because the incorporation of a second metal is an effective approach for tailoring electronic and geometric properties, optimizing the catalytic performance. Specially, amorphous alloys,⁴⁻⁵ as a relatively young class of materials with short-range order and long-range disorder, have shown promising catalytic performances in many hydrogenation reactions (e.g., selective hydrogenation of diene, selective hydrogenation of benzene,⁶ hydrogenation of sulfolene⁷ and hydrodesulphurization of dibenzothiophene⁸). In addition, Yamashita et al.⁹ reported that amorphous alloys have much higher catalytic activity than that of alloys in the crystallized state, resulting from the active site number and electronic state of surface metals. However, previous studies mainly focused on monometallic alloys with non-metallic elements (e.g., Ni-B amorphous alloy⁶), and very few reports⁷⁻⁸ show bimetallic amorphous catalysts. The reason can be explained as follows: for the two completely-fused metal elements in phase diagram (e.g., Pd and Pt¹⁰⁻¹¹), they are apt to form crystallized but not amorphous alloy; while in the case of two incompletely- or non-fused metal elements (e.g., Pd and Rh), it's rather difficult to obtain amorphous alloys based on conventional methods. Taking into account the unique merits of amorphous alloys, how to fabricate bimetal amorphous alloys with promising behaviour in heterogeneous catalysis is of vital importance and remains a great challenge.

Herein, we report the synthesis of monodispersed PdRhP amorphous alloy nanoparticles (NPs) via co-reduction of Pd(acac)₂ and Rh(acac)₃, employing trioctylphosphine (TOP) as stabilizer. The XRD pattern and HRTEM image confirm the amorphous structure feature of alloy NPs with mean size of 5.2±0.4 nm, and the aberration-corrected scanning transmission electron microscopy with energy dispersive X-ray mapping-scan (STEM-EDS) further demonstrates the uniform distribution of Pd, Rh and P element in each amorphous particle. The catalytic performances of PdRhP amorphous alloy NPs are investigated in

the chemoselective hydrogenation of various alkynes. Interestingly, a large selectivity toward various alkenes is obtained in a few hours with a high conversion (up to 100%) under quite mild reaction conditions (atmosphere pressure and 35 °C), which is superior to their single counterparts and shows promising applications in catalysis.

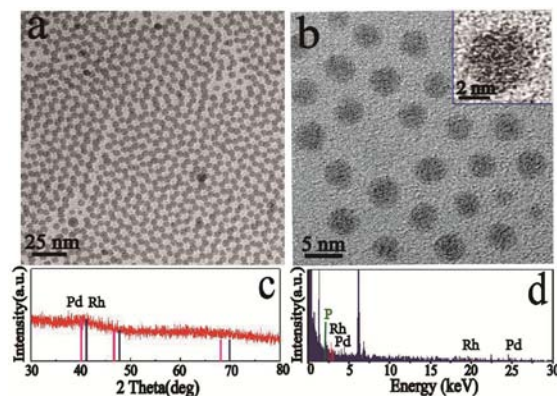


Fig. 1 (a) TEM image of the alloy NPs, (b) HRTEM image of the amorphous alloy NPs (inset: enlarged HRTEM image), (c) XRD pattern and (d) EDX spectrum of the alloy NPs.

Uniform alloy NPs with an average size of 5.2±0.4 nm were successfully synthesized in high yield (the detailed experimental procedure is described in the ESI), which are arranged regularly just like a decorative pattern (Fig. 1a). No distinct reflection corresponding to crystalline phases can be observed in the XRD pattern, in addition to one broad peak at 2θ ~45° (Fig. 1c), which is rather different from single crystalline Pd or Rh NPs (Fig. S1). This indicates the formation of amorphous alloy structure. Moreover, despite the signal of Pd and Rh element both can be captured (Fig. 1d), no lattice fringe image can be detected for the alloy NPs via the HRTEM technology as well (Fig. 1b, inset). Both the typical features above confirm an amorphous state of the alloy NPs.

In order to study the distribution of these two metal elements, the high-angle annular dark-field scanning transmission electron microscopy (HAADF-STEM) was used to make a further analysis (Fig. 2a). The energy dispersive X-ray (EDX) mapping-scan recorded through the single nanoparticle in the red square 75 frame (Fig. 2a) show a similar element distribution for Pd and Rh

(Fig. 2b). The line-scan spectra of Pd and Rh which were collected through the center of an individual nanoparticle (marked by the red line in Fig. 2a) also show rather similar behavior for Pd and Rh, demonstrating a homogeneous dispersion of these two species in an individual particle. This was further verified by detecting more than ten nanoparticles (Fig. 2c).

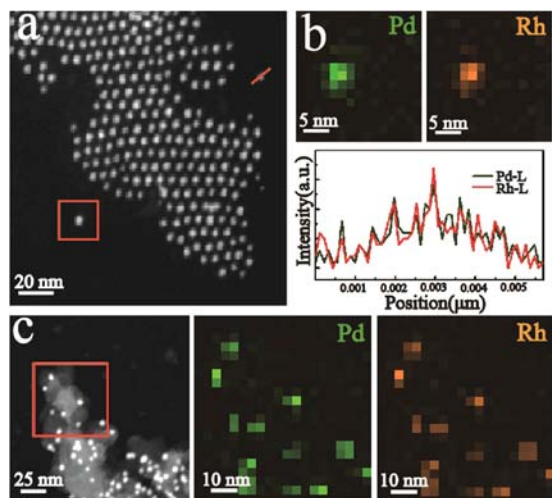


Fig. 2 (a) HAADF-STEM image of the alloy NPs, (b) EDX mapping image and line scanning results of an individual alloy particle, (c) mapping image of few alloy NPs supported on SiO₂. Green: Pd-L, yellow: Rh-L.

Moreover, it is worth noting that a strong P element signal can also be detected in the NPs (Fig. 1d), suggesting P may participate in the formation of amorphous alloy structure. We further performed elemental analysis for the amorphous alloy as listed in Table S1. The results demonstrate the existence of P with a molar percentage of 27%. This was further confirmed by HAADF-STEM-EDS technique (Fig. S2), and a uniform inter-distribution of Pd, Rh, P can be observed throughout the whole amorphous nanoparticles by the EDX-mapping scan. Fig. S3 displays the XRD patterns of alloy materials synthesized with various P/metal ratio, and it was found that the amorphous phase can only form at a high level of nominal P/metal ratio (14/1, Fig. S3A). Therefore, it can be concluded that the as-synthesized amorphous alloy is a ternary system (denoted as Pd₃₄Rh₃₉P₂₇).

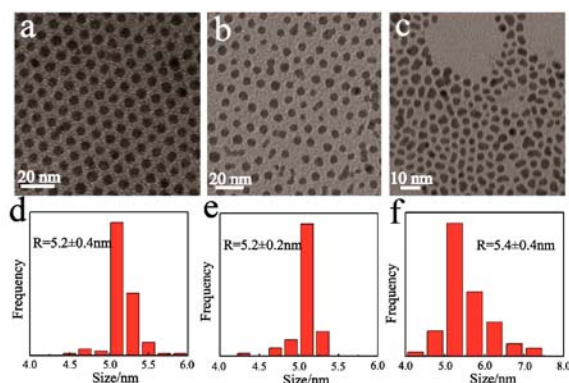


Fig. 3 TEM images of (a) Pd-Rh-P, (b) Rh, (c) Pd NPs with corresponding size distributions.

The semihydrogenation of alkyne plays a key role in industry because alkyne impurities in the olefin feed stocks will

lead to the deactivation of the polymerization catalyst.¹²⁻¹³ Pd is regarded as the best active component toward this reaction. As a result, the selective hydrogenation of alkynes was employed as the model reaction to evaluate the catalytic performance of alloy amorphous alloy. For comparison, pristine Rh and pristine Pd NPs with close size (~5.2 nm) were prepared by regulating the temperature and the amount of capping agent with the same method (Fig. 3). Commercial Rh/C and Pd/C were also employed as contrast catalysts. The concentration of each catalyst was determined so as to ensure the same noble metal content for all these catalyst samples. The hydrogenation of a model alkyne, phenylacetylene, was carried out at quite low temperature (35 °C) and atmosphere pressure. Fig. 4a shows the composition variation of the reaction mixture over the alloy amorphous catalyst at different point-in-time. The content of phenylacetylene decreases gradually in the whole reaction time range (3 h), while the styrene content increases rapidly firstly and reaches a maximum (100% conversion with 82% selectivity) at 2.5 h following by a sharp decrease from 2.5 to 3.0 h (Fig. 4a), exhibiting the well-known behaviour of consecutive reactions. Ethylbenzene, the complete hydrogenation product consists of a slow increase (0-2.5 h) and a fast enhancement (2.5-3.0 h). The best yield (82%) for styrene can be achieved at 2.5 h (Fig. 4b).

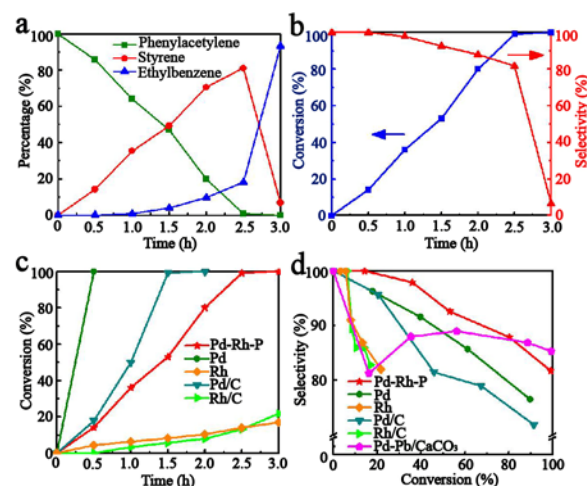


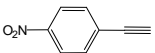
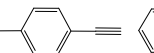
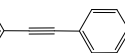
Fig. 4 (a) Product distribution of phenylacetylene hydrogenation as a function of reaction time over the bimetallic amorphous catalyst. (b) The conversion of phenylacetylene and selectivity for styrene in the reaction time range 0-3.0 h. (c) The phenylacetylene conversion as a function of time over various catalysts, with the metal amount of 0.16 μmol. (d) The styrene selectivity vs phenylacetylene conversion over various catalysts with the following metal content: Pd₃₄Rh₃₉P₂₇: 0.16 μmol; Pd: 0.08 μmol; Rh: 0.16 μmol; Pd/C: 0.08 μmol; Rh/C: 0.16 μmol; Pd-Pb/CaCO₃: 0.08 μmol.

In contrast, single Pd NPs and Pd/C show rather high catalytic activity: phenylacetylene completely transforms to ethylbenzene quickly in less than one hour and a half (Fig. 4c). The Pd NPs shows a slightly higher selectivity than Pd/C at various conversion levels, but both of them are lower than the selectivity of Pd₃₄Rh₃₉P₂₇ NPs (Fig. 4d). For Rh catalysts, both the Rh NPs and Rh/C sample display rather low conversion in the whole reaction duration (0-3.0 h), accompanying with dramatically decreased selectivity with the increase of conversion (0-20%). For comparison, the Lindlar Pd-Pb/CaCO₃ catalyst was

also evaluated (Fig. 4d), which displays a maximum olefin yield of 86.7%, close to the previous report.¹⁴ The Pd₃₄Rh₃₉P₂₇ catalyst in this work shows a close maximum yield to the Lindlar Pd-Pb/CaCO₃ one, indicating a similar bimetal action mechanism for the improved catalytic performance.¹⁵⁻¹⁶ Therefore, it is concluded that the PdRhP amorphous alloy exhibits significantly superior activity and selectivity to their single counterparts (pristine Pd or Rh catalyst).

Since some previous studies¹⁷⁻¹⁹ showed that the high catalytic activity of nanoparticles might owe to molecular species leaching from the nanoparticles, we made a filtration test to discuss this issue. The hydrogenation of phenylacetylene reaction catalyzed by alloy NPs was terminated after 1 h at a conversion of 81% (Fig. S4), then the H₂ pressure was released and the nanoparticles were removed by centrifugation. Subsequently, the filtrate was replaced into the flask to restart the reaction under the same conditions for one hour. No obvious change in the mixture composition was observed, except a rather slight increase in the phenylacetylene conversion which might be due to the residual catalyst in the filtrate. This suggests that the alloy NPs are responsible for the catalytic activity. The cycle ability of alloy NPs was also explored by employing the selective hydrogenation of phenylacetylene. The catalyst was separated by centrifugation, washed and reused without further treatment. After five recycles, the conversion of phenylacetylene still remained 100% and no obvious change in the product composition was found (Fig. S5). From the viewpoint of practical applications, supporting nanocatalysts on a carrier is highly significant for improving stability, separation and recycling.²⁰ This is under investigation in our lab.

Table 1 Selective hydrogenation reaction of various alkynes

Substrates					
Catalyst	Time(h)	Con.(%)	Sel.(%) ^a	Con.(%) Sel.(%) ^b	Con.(%) Sel.(%) ^c
Pd ₃₄ Rh ₃₉ P ₂₇	4	100	99.2	100 91.9	99.3 54.9 <i>cis</i>
	2.5	78.6	98.6	67.2 93.3	73.5 77.9 <i>cis</i>
	1.5	44.4	94.7	38.5 95.5	40.1 72.9 <i>cis</i>
Pd	4	100	0	100 84.7	99.4 57.1 <i>cis</i>
	2.5	86.3	73.7	83.1 80.5	82.8 61.8 <i>cis</i>
	1.5	45.9	81.5	39.9 87.2	51.7 69.4 <i>cis</i>
Pd/C	4	100	0	62.5 88.9	99.4 55.2 <i>cis</i>
	2.5	76.9	83.9	48.7 95.7	76.5 66.4 <i>cis</i>
	1.5	38.7	87.3	26.8 93.2	47.7 74.2 <i>cis</i>
Rh/C	Rh/C	0	0	12.6 81.4	25.2 78.3 <i>cis</i>

Reaction conditions: dioxane (1 ml), 1 bar H₂, 35 °C. ^aSelectivity for 1-ethenyl-4-nitrobenzene; ^bselectivity for 4-bromostyrene; ^cselectivity for (Z)-stilbene.

Furthermore, the ternary amorphous alloy also exhibits excellent catalytic performance toward selective hydrogenation of other alkynes, and the results are given in Table1. For 4-nitroethynylbenzene hydrogenation, a high selectivity 94.7% (at 44.4% conversion) for olefin is obtained over Pd₃₄Rh₃₉P₂₇ alloy, which keeps at a high level (99.2% selectivity) even at 100% conversion. However, a relatively low selectivity or quite low activity is observed over single Pd (81.5% selectivity at 45.9%

conversion) or Rh catalyst, respectively. In the case of 4-bromostyrene hydrogenation, the Pd₃₄Rh₃₉P₂₇ NPs display rather satisfactory catalytic behavior both at low and high conversions (95.5% selectivity at 38.5% conversion; 91.9% selectivity at 100% conversion), in comparison with monometallic Pd or Rh catalyst. Hydrogenation of tolane was also investigated. The Pd₃₄Rh₃₉P₂₇ (72.9% selectivity at 40.1% conversion) and pristine Pd (69.4% selectivity at 51.7% conversion) catalysts reveal rather close catalytic behavior in this reaction; while the Rh/C sample shows the highest selectivity for (Z)-stilbene (78.3%) but rather low conversion (25.2%). These results above demonstrate that Pd₃₄Rh₃₉P₂₇ displays largely enhanced catalytic performance toward selective hydrogenation of various alkynes compared with pristine Pd or Rh catalyst.

Based on the results above, it can be seen that the pristine Pd catalyst shows limited selectivity, in accordance with the previous reports.²¹⁻²² This can be possibly attributed to the formation of hydride phase which is active in over-hydrogenation reactions.²³ The employment of second element is the main strategy to improve performances of Pd catalysts (e.g., Pd-Ga,²⁴ Pd-Cu,²⁵ Pd-Ni¹² and Pd-Si²⁶). The presence of other metals or metalloids would modify the geometric effect and electron density of Pd atom, which influence the adsorption behavior of reactants and intermediates.²⁷

In this work, the presence of Rh and P element in the PdRhP amorphous alloy may function by a similar way (e.g., the geometric and electronic modification effect of Rh and P element^{12,24,28}) to improve the hydrogenation selectivity of alkyne. On the other hand, the inherent nature of amorphous alloy may also impose unique influence on the enhanced selectivity. From a theoretical point of view, the metalloid element in amorphous alloy could change the coordination environment of active metal (e.g., in NiB system²⁹), and the short range order between neighboring metal atoms would influence the adsorption of reactants.³⁰ Therefore, the improved catalytic performance of PdRhP can be attributed to the intrinsic nature of amorphous alloy with modified geometric/electronic structure, which will be studied in our future work.

In summary, this work provides a facile method for the preparation of ternary PdRhP amorphous alloy NPs with uniform particle size. The combination of Pd and Rh with the presence of P shows excellent catalytic performances toward hydrogenation of several alkynes under mild reaction conditions, in comparison with pristine Rh or Pd catalyst. This approach can be extended to other amorphous bimetallic alloys with superior catalytic behavior and potential applications in industrial hydrogenation reactions.

Acknowledgements

This work was supported by the 973 Program (Grant no. 2011CBA00504), the National Natural Science Foundation of China (NSFC), the Scientific Fund from Beijing Municipal Commission of Education (20111001002) and the Fundamental Research Funds for the Central Universities (ZD 1303). M. Wei particularly appreciates the financial aid from the China National Funds for Distinguished Young Scientists of the NSFC.

Notes and references

State Key Laboratory of Chemical Resource Engineering, Beijing University of Chemical Technology, Beijing, P. R. China. Fax: (+) 86-10-64425385; E-mail: weimin@mail.buct.edu.cn; shixx@mail.buct.edu.cn

- 1 P. Rodriguez, F. D. Tichelaar, M. T. M. Koper and A. I. Yanson, *J. Am. Chem. Soc.*, 2011, **133**, 17626-17629.
- 2 S. Zafeirotas, S. Piccinin and D. Teschner, *Catal. Sci. Technol.*, 2012, **2**, 1787-1801.
- 3 E. C. Corbos, P. R. Ellis, J. Cookson, V. Briois, T. I. Hyde, G. Sankar and P. T. Bishop, *Catal. Sci. Technol.*, 2013, **3**, 2934-2943.
- 4 Z. Jiang, H. Yang, Z. Wei, Z. Xie, W. Zhong and S. Wei, *Appl. Catal. A*, 2005, **279**, 165-171.
- 5 Y. Chen, B. Liaw and S. Chiang, *Appl. Catal. A*, 2005, **284**, 97-104.
- 6 (a)M. Shapaan, A. Bárdos, L. K. Varga and J. Lendvai, *Mater. Sci. Eng., A*, 2004, **366**, 6-9; (b)H. E. Schone, H. C. Hoke, A. Johnson, *Mater. Sci. Eng.*, 1988, **97**, 431-435; (c)Y. Ma, W. Li, M. Zhang, Y. Zhou and K. Tao, *Appl. Catal. A*, 2003, **243**, 215-223; (d)H. Li, D. Chu, J. Liu, M. Qiao, W. Dai and H. Li, *Adv. Synth. Catal.*, 2008, **350**, 829-836.
- 7 H. Li, D. Chu, J. Liu, M. Qiao, W. Dai and H. Li, *Adv. Synth. Catal.*, 2008, **350**, 829-836.
- 8 L. Song, W. Li, G. Wang, M. Zhang and K. Tao, *Catal. Today*, 2007, **125**, 137-142.
- 9 H. Yamashita, M. Yoshikawa, T. Funabiki and S. Yoshida, *J. Chem. Soc.*, 1986, **82**, 1771-1780.
- 10 H. Zhang, M. Jin, H. Liu, J. Wang, M. J. Kim, D. Yang, Z. Xie, J. Liu and Y. Xia, *ACS Nano*, 2011, **5**, 8212-8222.
- 11 X. Huang, Y. Li, Y. Li, H. Zhou, X. Duan and Y. Huang, *Nano. Lett.*, 2012, **12**, 4265-4270.
- 12 S. Domínguez-Domínguez, Á. Berenguer-Murcia, D. Cazorla-Amorós and Á. Linares-Solano, *J. Catal.*, 2006, **243**, 74-81.
- 13 F. M. McKenna, L. Mantarosie, R. P. K. Wells, C. Hardacre and J. A. Anderson, *Catal. Sci. Technol.*, 2012, **2**, 632-638.
- 14 T. A. Nijhuis, G. van Koten and J. A. Moulijn, *Appl. Catal. A*, 2003, **238**, 259-271.
- 15 P. W. Albers, K. Möbus, C. D. Frost and S. F. Parker, *J. Phys. Chem. C*, 2011, **115**, 24485-24493.
- 16 F. M. McKenna, R. P. K. Wells and J. A. Anderson, *Chem. Commun.*, 2011, **47**, 2351-2353.
- 17 L. D. Pachón and G. Rothenberg, *Appl. Organomet. Chem.*, 2008, **22**, 288-299.
- 18 J. S. Chen, A. N. Vasiliev, A. P. Panarello and J. G. Khinast, *Appl. Catal. A*, 2007, **325**, 76-86.
- 19 S. S. Soomro, F. L. Ansari, K. Chatziapostolou and K. Köhler, *J. Catal.*, 2010, **273**, 138-146.
- 20 (a)M. Comotti, W. C. Li, B. Spliethoff and F. Schüth, *J. Am. Chem. Soc.*, 2006, **128**, 917-924; (b)L. N. Protasova, E. V. Rebrov, K. L. Choy, S. Y. Pung, V. Engels, M. Cabaj, A. E. H. Wheatley and J. C. Schouten, *Catal. Sci. Technol.*, 2011, **1**, 768-777; (c)N. Lopez, J. K. Nørskov, T. V. W. Janssens, A. Carlsson, A. Puig-Molina, B. S. Clausen and J.-D. Grunwaldt, *J. Catal.*, 2004, **225**, 86-94; (d)S. Domínguez-Domínguez, Á. Berenguer-Murcia, Á. Linares-Solano and D. Cazorla-Amorós, *J. Catal.*, 2008, **257**, 87-95.
- 21 C. A. Hamilton, S. D. Jackson, G. J. Kelly, R. Spence and D. Bruin, *Appl. Catal. A*, 2002, **237**, 201-209.
- 22 J. Osswald, R. Giedigkeit, R. E. Jentoft, M. Armbrüster, F. Girgsdies, K. Kovnir, T. Ressler, Y. Grin and R. Schlögl, *J. Catal.*, 2008, **258**, 210-218.
- 23 (a)D. Teschner, J. Borsodi, A. Wootsch, Z. Révay, M. Hävecker, A. Knop-Gericke, S. D. Jackson and R. Schlögl, *Science*, 2008, **320**, 86-89; (b)N. López and C. Vargas-Fuentes, *Chem. Commun.*, 2012, **48**, 1379-1391; (c)M. García-Motaa, B. Bridier, J. Pérez-Ramírez and N. López, *J. Catal.*, 2010, **273**, 92-102.
- 24 G. Wowsnick, D. Teschner, M. Armbrüster, I. Kasatkin, F. Girgsdies, Y. Grin, R. Schlögl and M. Behrens, *J. Catal.*, 2014, **309**, 221-230.
- 25 M. B. Boucher, B. Zugic, G. Cladaras, J. Kammert, M. D. Marcinkowski, T. J. Lawton, E. C. H. Sykes and M. Flytzani-Stephanopoulos, *Phys. Chem. Chem. Phys.*, 2013, **15**, 12187-12196.
- 26 R. Tschan, R. Wandeler, M. S. Schneider, M. M. Schubert and A. Baiker, *J. Catal.*, 2001, **204**, 219-229.
- 27 D. Mei, M. Neurock and C. M. Smith, *J. Catal.*, 2009, **268**, 181-195.
- 28 (a)A. M. Alexander and J. S. J. Hargreaves, *Chem. Soc. Rev.*, 2010, **39**, 4388-4401; (b)B. Rajesh, N. Sasirekha, Y. W. Chen, *J. Mol. Catal. A: Chem.*, 2007, **275**, 174-182; (c)S. Carencu, A. Leyva-Pérez, P. Concepción, C. Boissière, N. Mézailles, C. Sanchez and A. Corma, *Nano Today*, 2012, **7**, 21-28.
- 29 H. Li, J. Zhang, H. Li, *Catal. Commun.*, 2007, **8**, 2212-2216.
- 30 (a)M. Crespo-Quesada, J. M. Andanson, A. Yarulin, B. Lim, Y. Xia and L. Kiwi-Minsker, *Langmuir*, 2011, **27**, 7909-7916; (b)A. M. Alexander and J. S. J. Hargreaves, *Chem. Soc. Rev.*, 2010, **39**, 4388-4401; (c)S. Yoshida, H. Yamashita, T. Funabiki and T. Yonezawa, *J. Chem. Soc., Faraday Trans. 1*, 1984, **80**, 1435-1446; (d)H. Yamashita, M. Yoshikawa, T. Funabiki and S. Yoshida, *J. Chem. Soc., Faraday Trans. 1*, 1985, **81**, 2485-2493.